Sustainability in Environment
ISSN 2470-637X (Print) ISSN 2470-6388 (Online)
Vol. 10, No. 2, 2025
www.scholink.org/ojs/index.php/se

Original Paper

Mechanistic Study of Citrate Affecting the Adsorption of Gold Nanoparticles by Goethite

Shanshan Zhang[a], YuHong Fu[a*] Zhimei Jiang[a], Yun Wang[a], Shanshan Li[b], Sen Li[a], & Shuai Zhang[a]

[a] School of Geography and Environmental Sciences, Guizhou Normal University, Guiyang 550025, China

[b] School of Chemistry and Materials Science, Guizhou Normal University, Guiyang 550025, China

[*] Corresponding author

Received: April 29, 2025 Accepted: May 28, 2025 Online Published: June 11, 2025

doi:10.22158/se.v10n2p143 URL: http://dx.doi.org/10.22158/se.v10n2p143

Abstract

The mechanism of regulating the interfacial behavior of gold nanoparticles (AuNPs) in environmental media is key to assessing their ecological risks. In this study, we break through the traditional one-factor adsorption research model and focus on the multiscale regulatory role of Citrate (Cit) in the nanoparticle-mineral interface, revealing for the first time the biphasic mechanism by which this molecule dominates the environmental behavior of AuNPs through pH-responsive coordination mode switching. By constructing the goethite-AuNPs- Cit ternary interface model, it was found that : under acidic conditions (pH < pHpzc), Cit competes for positively charged adsorption sites on the surface of goethite with the AuNPs and inhibits the adsorption significantly; whereas under alkaline conditions (pH > pHpzc), Cit bridges the negatively charged clinoptilolite and AuNPs through charge-assisted hydrogen bonds (CAHBs) and Lewis acid-base interactions, promoting adsorption. This study innovatively established an organic ligand-mediated dynamic regulation model of nanoparticles (NPs) interface, clarified the mutation mechanism of NPs 'retardation-migration' behavior caused by pH oscillation in rhizosphere microenvironment, and provided a theoretical basis for the study of the interaction between NPs and minerals. Meanwhile, it will also bring new insights into the environmental fate of AuNPs, especially in the rhizosphere environment.

Keywords

Gold nanoparticles, Goethite, Interface bridging, Environmental fate, Adsorption

1. Introduction

Nanoparticles (NPs) have demonstrated tremendous potential in diverse fields including catalysis,

environmental protection, materials science, and biomedicine, owing to their small-size effects and surface reactivity (Huang, Fan, Dong, Wang, Yang, X. C., & Yang, S. M., 2017; Chen & Feng, 2022; Zhang, Cong, Huang, & Du, 2019; Li, Yang, Xu, Wang, Zhang, & Wei, 2022). Taking gold nanoparticles (AuNPs) as an example, their advantages such as facile synthesis (Staroverov, Vyrshchikov, Bogatyrev, & Dykman, 2024) controllable size and morphology (Cai, Li, Gu, Zhou, & Zhao, 2021), excellent biocompatibility (Kus-Liskiewicz, Fickers, & Ben, 2021), and unique optical properties (Zhang, McKelvie, Cattrall, & Kolev, 2016) have enabled widespread applications in bio-electrochemical sensors (Koc, Benam, Aral, Shahbazi, & Ulubayram, 2024), optical/electrochemical probes (Fernandez-Lopez, Polavarapu, Solis, Taboada, & Obelleiro, 2015), bioimaging (Wu, Ali, Chen, Fang, & El-Sayed, 2019) and drug delivery systems (Dykman, Khlebtsov, & Khlebtsov, 2025). However, during their migration and fate in terrestrial environments, AuNPs can significantly modulate the distribution behaviors of hazardous heavy metals, metalloids, radionuclides, and organic contaminants (Hochella, Mogk, Ranville, Allen, Luther, Marr, McGrail, Murayama, Qafoku, Rosso et al., 2019). Furthermore, substantial environmental release of AuNPs may alter their bioavailability through aggregation and adsorption processes, thereby posing ecological risks (Stevenson, Dickson, Klanjscek, Keller, McCauley, & Nisbet, 2013; Abbas, Yousaf, Ullah, Ali, Ok, & Rinklebe, 2020). Consequently, elucidating the interfacial behaviors of AuNPs in environmental matrices becomes crucial for risk assessment.

As the reactive minerals of highly abundance in soil, the surface charge properties (pHpzc range 4.8-8.5) of iron (hydrogen) oxides (e.g., goethite, hematite) are closely related to the sorption behavior of NPs (Abbas, Yousaf, Ullah, Ali, Ok, & Rinklebe, 2020). Goethite is the most common iron (hydrogen) oxides in an aqueous environment with abundant and highly reactive surface functional groups, and its chain structure exposes functional groups with near-neutral pHpzc (~6.7), giving it a strong adsorption capacity for charged NPs over a wide pH range (Hanlie, Qinyan, Jianping, Shirong, Ruizhong, 1999; Wu, Ye, Li, Sun, Huang, Liu, Ahmed, & Wu, 2023). It has been shown that iron (hydrogen) oxides can immobilize NPs by electrostatic interaction, ligand bonding and other mechanisms, but most existing researches ignore the modulating effect of co-existing organic ligands such as Cit (Smith, Pike, Kelly, Nason, 2015; Zhao, Liu, Wang, Cao, & Xing, 2015).

Low molecular weight organic acids (e.g., Cit) are prevalent in soil, and the negative charges generated by the carboxyl dissociation can significantly alter mineral surface properties (Zhu, Fu, Qiu, Liu, Hu, Huang, &Violante, 2019). Notably, Cit is not only a commonly used stabilizer in the synthesis of NPs but may also affect NPs-mineral interactions through competitive adsorption or interfacial bridging [26,27]. However, previous studies (e.g., Enzweiler (Enzweiler & Joekes, 1992), Smith (Smith, Yang, Bitter, Ball, & Fairbrother, 2012), etc.), although using Cit for the synthesis of AuNPs, removed Cit residues in adsorption experiments, leading to a long period of neglect of its potential effects.

In this study, we focused on the regulatory mechanism of Cit on the adsorption of AuNPs by goethite, and designed pH, ionic strength (IS) and Cit concentration gradient experiments to elucidate (1) the

competitive or synergistic adsorption behaviors of Cit under different pH conditions, and (2) the mechanism of Cit-mediated interaction at the NPs-mineral interface. The results of the study will fill the cognitive gap of the dynamic role of Cit in the environmental fate model of NPs and provide theoretical support for the prevention and control of nano-pollution in organic acid-enriched regions such as inter-roots.

2. Materials and Methods

2.1 Experimental Reagents

We obtained a 1%, w/w sodium Cit aqueous solution from Chongqing Chuan Dong Chemical Company, $HAuCl_4$ aqueous solution (0.01%, w/w) was purchased from Aladdin Reagent Company, Au standard solution (100 μg/mL) was purchased from the National Center for Analysis and Testing of Nonferrous Metals and Electronic Materials, $FeCl_3-6H_2O$ (analytically pure), HNO_3 (analytically pure), NaOH (analytically pure), $FeCl_3·6H_2O$ (analytically pure), HNO_3 (analytically pure), NaOH (analytically pure), HCl (analytically pure) were acquired from Chongqing Chuan Dong Chemical Company, 0.45 μm PTFE membrane was purchased from Tianjin Jinteng Experimental Equipment Co. Anhydrous ethanol was bought from Tianjin Komeo Chemical Reagent.

2.2 Synthesis and Pretreatment of AuNPs

AuNPs with a molar ratio (citrate: $HAuCl_4$) of 4.65 were synthesized using the classical Frens method, and it was concluded that the stability of nanogold at this molar ratio was better (Fu, Wan, Qin, Nie, Yu, & Li, 2020; Frens, 1973).The specific synthesis steps are as follows: under the conditions of condensation reflux and magnetic stirring, 21 mL of aqueous sodium Cit solution (1%, w/w) was added rapidly to boiling 600 mL of aqueous HAuCl4 solution (0.01%, w/w) (1%, w/w), continued heating for 20 min and then stopped, kept the condensation reflux, cooled to room temperature and then put in 4 ℃ refrigerator for storage. The synthesized AuNPs colloids showed a clear burgundy color. The particle size and dispersion of AuNPs were detected using a Malvern Zetasizer (Nano ZS90, Malvern, UK). using a flame atomic absorption spectrophotometer (AAS, GGX-800, Hai Guang, China) to test the concentration of gold in the colloid of AuNPs was tested.

Sodium Cit was utilized as a dual-purpose agent in the synthesis of AuNPs, serving both as a reducing agent and a stabilizer. Following the synthesis of AuNPs colloids, there remained a significant excess of Cit, with a concentration of approximately 292~300 mg/L. To study the effect of Cit on the adsorption behaviors of goethite and nano-gold, the concentration of Cit needs to be controlled, so the AuNPs colloids should be pretreated as follows: centrifugation of the AuNPs colloid at 12000 rpm for 35 min. Following the centrifugation process, the supernatant was partially removed, and an equal volume of pure water was added and thoroughly mixed. The concentration of Cit in the treated colloid was measured to be 148 mg/L using high-performance liquid chromatography (HPLC, LC-2030, Shimadzu, Japan). When almost all the supernatant was replaced with pure water, the Cit concentration was 15 mg/L as measured by HPLC. the Cit concentrations were obtained as ~300, ~150, and ~15

mg/L of AuNPs colloids (numbered Au-300, Au-150, and Au-15, respectively). Using a UV-vis spectrophotometer (UV-vis, CARY 300, Agilent, Santa Clara, CA, USA) to test the UV-Vis absorption spectra of treated and untreated AuNPs. Malvern Zetasizer was used to test the Zeta potential of treated and untreated AuNPs.

2.3 Synthesis of Goethite

Goethite was synthesized using a classical hydrothermal method in the following manner (Dhakal, Coyne, McNear, Wendroth, Vandiviere, D'Angelo, & Matocha, 2021). 50 mL of $FeCl_3 \cdot 6H_2O$ (0.2 mol/L) solution was added to a 1 L polyethylene flask, then 90 mL of NaOH (5 mol/L) solution was added to the flask, and the suspension was diluted with deionized water to 1 L. The flask was sealed and placed in a 70 ℃ water bath for 60 hours. Once the mixture had cooled down to the temperature of the room, it was passed through a 0.45 μm PTFE membrane using filtration. The resulting mixture was then rinsed three times with purified water and twice with anhydrous ethanol. Finally, it was left to dry overnight at a temperature of 40 ℃. The solid obtained from the drying was ground and stored under dry conditions. The physical phase and microstructure of the synthesized goethite were characterized using X-ray diffraction (XRD, Empyrean, PANalytical B.V, NL) and scanning electron microscopy (SEM, Scios, FEI, USA). We analyzed the specific surface area of goethite using the Autosorb-iQ2-MP gas adsorption analyzer from Quantachrome, based in the USA. The Zeta potential of goethite was measured using the Malvern Zetasizer.

2.4 Batch Adsorption and Desorption Regeneration

(1) Batch adsorption experiments

Batch adsorption experiments were conducted to investigate the adsorption behavior of AuNPs on goethite surface under different Cit concentrations, pH and IS conditions. The IS of the AuNPs colloid was modified to 0.5 and 1.5 mM NaCl using a NaCl solution. Additionally, the initial pH of AuNPs colloid solution was adjusted to 4, 5, 6, 7, 8, 9, 10, and 11 using either HCl or NaOH solution. The ratio of goethite powder to AuNPs colloid in the adsorbent system was 0.1 g:20 mL, and the corresponding ratio of goethite powder to the colloidal solution was determined based on this solid-liquid ratio. The samples underwent oscillating in a constant temperature oscillator at a speed of 150 rpm and a temperature of 25 ℃. Following this, the solid-liquid separation was performed by filtering the samples through a 0.45 μm PTFE membrane. 1 ml of the filtrate was added to 1 ml of aqua regia for overnight digestion, and the concentration of un-adsorbed Au and the concentration of Cit in the supernatant were measured by AAS and HPLC, respectively. The solid samples after isolation of adsorption were quickly rinsed twice using an aqueous solution of HCl or NaOH at the same initial pH as the adsorption system, dried overnight at 40 °C, and then ground into a powder using an agate mortar. The resulting powder samples were characterized using SEM and Fourier transform infrared spectroscopy (Vertex 70, Bruker, Germany).

In order to delve deeper into the workings of the Cit adsorption system, an experimental study was conducted to examine the adsorption of Cit by goethite. The initial pH of Cit (300 mg/L) solution was

adjusted to 4, 5, 6, 7, 8, 9, 10, and 11 by HCl or NaOH solution, and the goethite powder was added to the solution at a solid-liquid ratio (0.1 g:20 mL). The samples were shaken at 150 rpm, 25 °C, and after sampling at time points, the samples were filtered using a 0.45 μm PTFE membrane, and the Cit concentration was measured using HPLC and the Au concentration was measured using AAS. Characterization of the samples at the end of adsorption was done using attenuated total reflection-FTIR (ATR-FTIR).

(2) Desorption regeneration cycle

The solid powder obtained after adsorption process was added to an aqueous solution of either HCl or NaOH, which had the same initial pH as the adsorption system. The ratio of solid to liquid was 0.1 g to 20 ml. The mixture was then placed in a thermostatic oscillator and set to oscillate at 150 rpm and 25 ℃. After sampling at specific time points, the mixture was filtered through a PTFE membrane with a pore size of 0.45 μm. Subsequently, 1 ml of the filtrate was combined with 1 ml of aqua regia to remove the Au concentration and Cit concentration in the filtrate overnight. Au concentration and Cit concentration in the filtrate were measured by using AAS and HPLC, respectively, to observe the desorption of AuNPs and Cit by goethite.

3. Results and Discussion

3.1 Characterization of AuNPs and Goethite

(1) Characterization of AuNPs

We utilized the Frens method to create AuNPs colloids in a rich burgundy hue. The molar ratio of sodium Cit to $HAuCl_4$ was carefully adjusted to 4.65, ensuring excellent stability of the colloids. The concentration of Au in the colloids was determined to be 60 mg/L using AAS. The Malvern Zetasizer test results showed that the average particle size of AuNPs was 19.23 nm, and the polydispersity coefficient was 0.091, which indicated that the particle size distribution was relatively uniform (Table 1). The absorption spectra of the pretreated AuNPs colloids closely resembled those of the untreated AuNPs (Figure 1), suggesting that the treatment method did not have a significant impact on the particle size and distribution. Based on the zeta potential test results, it was observed that the zeta potential values of Au-300 and Au-150 were similar. This indicates that the stability of Au-150 was not influenced by the treatment method. Additionally, it was found that the stability of Au-150 was not affected by the treatment method, and that the stability of Au-150 was not affected by the treatment method even with a decrease in Cit concentration, although the absolute value of Zate potential of Au-15 decreased slightly (Figure 2).

Table 1. AuNPs Particle Size

number of tests	particle size（nm）	polydispersity factor
1	19.31	0.096

2	19.27	0.092
3	19.04	0.100
4	19.31	0.076
average value	19.23	0.091

Note. serial numbers 1, 2, 3 and 4 are the results of four repetitions of the same AuNPs sample.

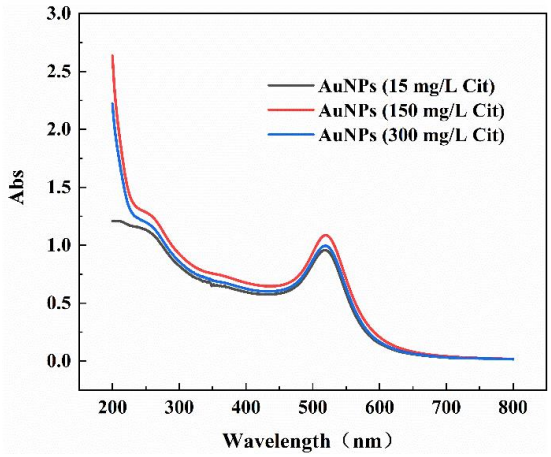

Figure 1. UV-Vis Absorbance Variation of AuNPs at Different Cit Concentrations

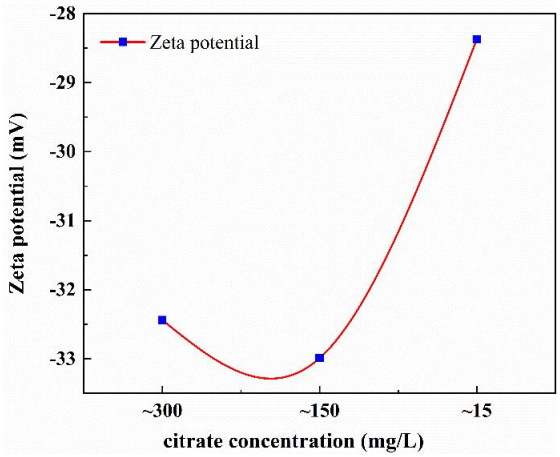

Figure 2. Zeta Potential of AuNPs at Different Cit Concentrations

(2) Characterization of goethite

Goethite was synthesized using the classical hydrothermal method resulting in a yellow powder with a specific surface area of 38.310 m^2/g. The goethite was analyzed using XRD and SEM. The XRD patterns of the synthesized goethite samples closely matched the goethite standard data (JCPDS card PDF file no. 81-0464) (Figure 3), suggesting that the synthesized sample is indeed goethite. The SEM image in Figure 4 displays the synthesized goethite sample, exhibiting a needle-like morphology that

aligns with the fundamental characteristics of goethite.

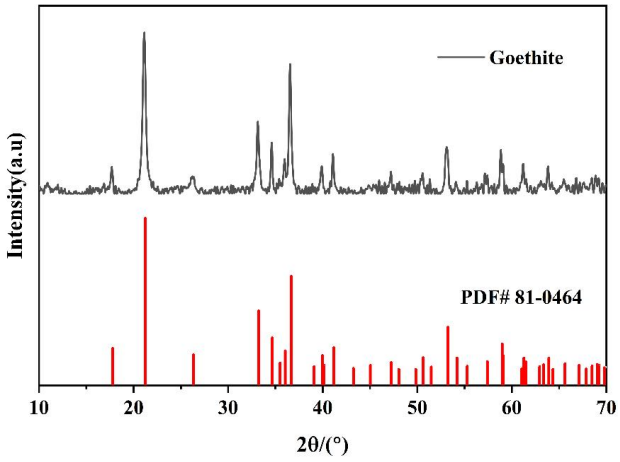

Figure 3. XRD Pattern of Goethite

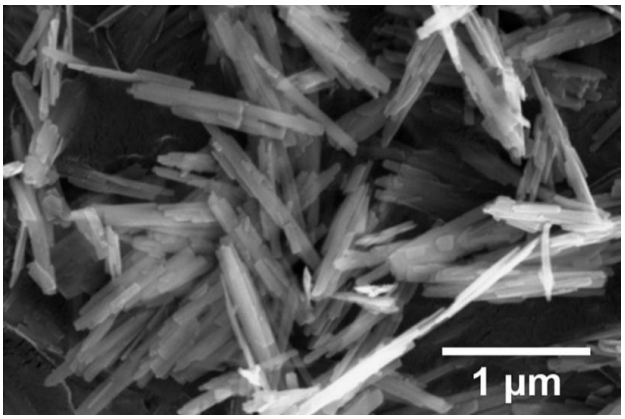

Figure 4. SEM Image of Goethite

Furthermore, when examining goethite as a mineral with variable charge, it becomes crucial to ascertain the isoelectric point of the mineral. This refers to the pH value at which the positive and negative charges on the surface of the particle's surface reach equilibrium. In this paper, the zeta potential of goethite in different pH solutions was measured to determine its isoelectric point, and the results are shown in Figure 5, which can be observed that its isoelectric point is between pH 8 and 9, after fitting, the isoelectric point of goethite is calculated to be about pH 8.6.

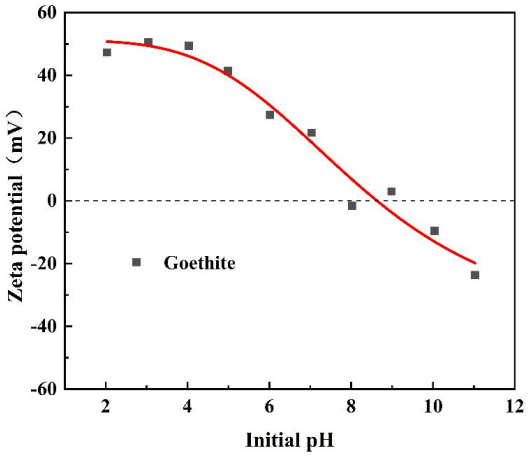

Figure 5. Zeta Potential of Goethite

3.2 Adsorption of AuNPs on Goethite

3.2.1 Adsorption of AuNPs-300 on Goethite

Under conditions with a Cit concentration of 300 mg/L and no NaCl addition (i.e., ionic strength (IS) is 0 mM NaCl) (Figure 6a), the adsorption rate of AuNPs on goethite reached its minimum (<20%) at an initial pH of 6, with no significant increase observed over the 20-day period. At pH 5 and 11, the adsorption rate was approximately 50% and exhibited an increasing trend over time. Under other pH conditions (4, 7, 8, 9, 10), the adsorption rate of AuNPs reached 100% within 24 hours. For IS = 0.5 mM NaCl (Figure 6b), within the initial pH range of 4–9 (experiments at pH 10 and 11 were omitted due to potential AuNPs aggregation caused by strong alkalinity and elevated IS; this applies to subsequent similar conditions), the adsorption rate of AuNPs remained lowest at pH 6, not exceeding 20% over 20 days. At pH 5, the adsorption rate increased from 20% to 50% over 20 days, while at pH 4, 7, 8, and 9, significant adsorption of AuNPs on goethite was observed. The adsorption behaviors under the two IS conditions exhibited similarities across varying initial pH levels, with detailed effects discussed later. Overall, the adsorption rates of AuNPs on goethite were lower at initial pH 5 and 6 but reached 100% within 24 hours under other pH conditions. SEM images of goethite after AuNPs adsorption (Figure 7) revealed that AuNPs were dispersed and uniformly adsorbed on the surface, with higher adsorption quantities observed in acidic (Figure 7a) and alkaline (Figure 7e) environments compared to the initial pH 6 condition (Figure 7c).

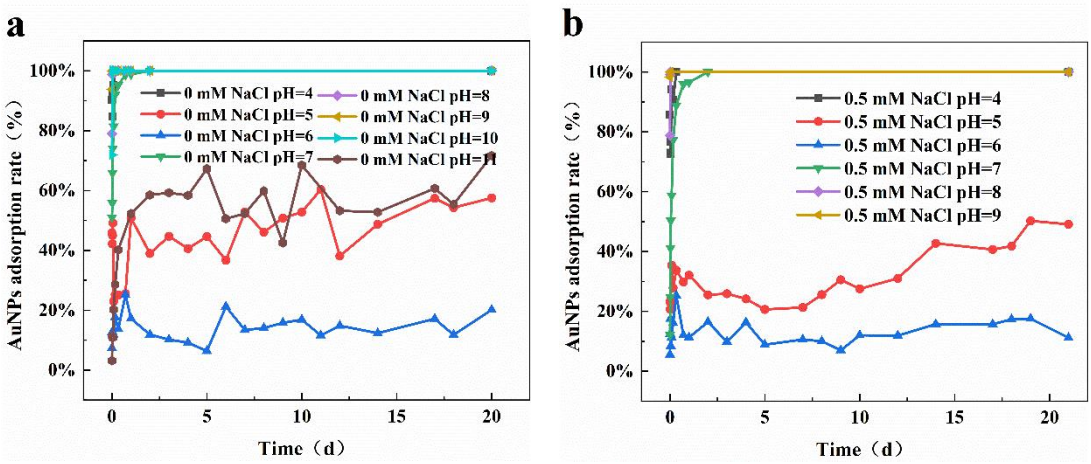

Figure 6. Adsorption Rate of AuNPs on Goethite over Time under Different Initial pH Values at a Cit Concentration of 300 mg/L: (a) 0 mM NaCl; (b) 0.5 mM NaCl.

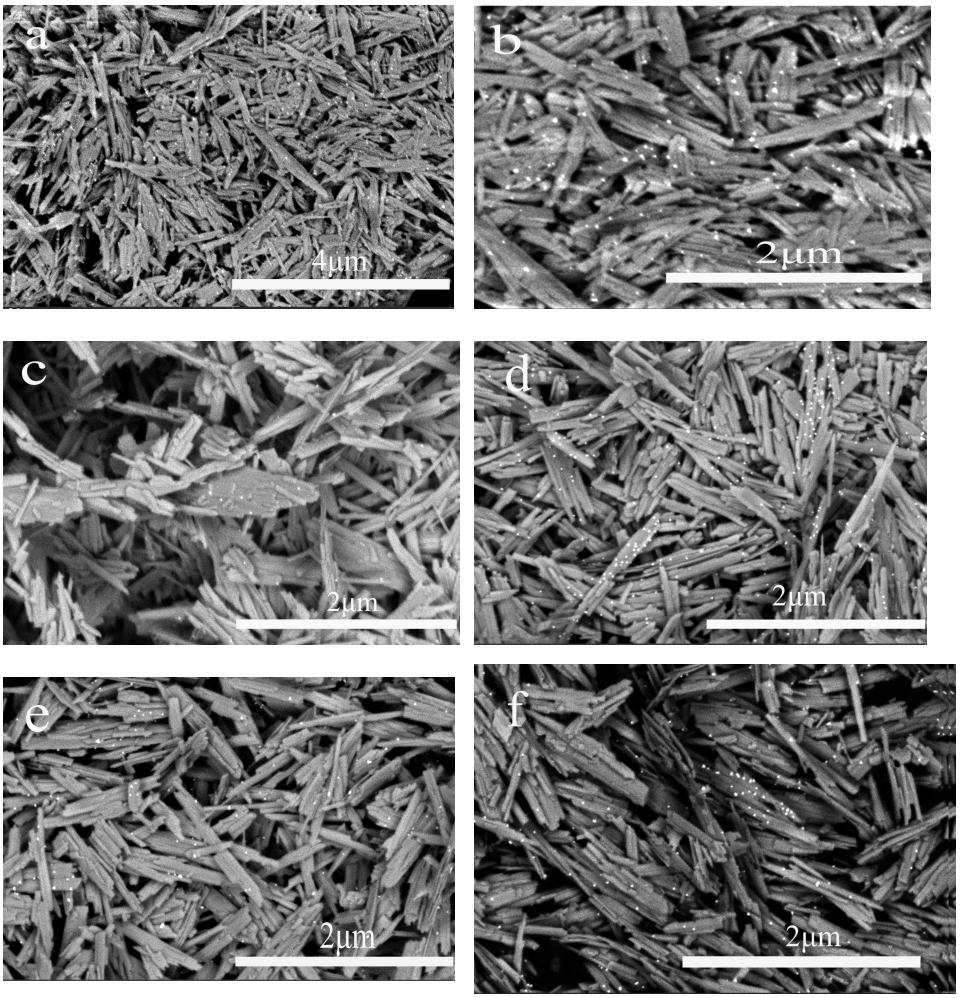

Figure 7. SEM Images of AuNPs Adsorbed by Goethite under Different Conditions

3.2.2 Adsorption of AuNPs-150 on Goethite

At a Cit concentration of 150 mg/L and IS = 0 mM NaCl (Figure 8a), the adsorption rates of AuNPs on goethite were lowest at initial pH 5 and 6, both below 20%. At pH 11, complete adsorption required 4 days, while at pH 4, adsorption initiated rapidly but reached 100% after 4 days. Under other pH conditions, the adsorption rate rapidly achieved 100%. For IS = 0.5 mM NaCl (Figure 8b), the lowest adsorption rates similarly occurred at pH 5 and 6 (20–40%). At pH 4, the adsorption behavior resembled that under 0 mM NaCl, with full adsorption achieved after 7 days. At other pH values, adsorption reached 100% within a brief time. Except for pH 11, the adsorption behavior of AuNPs on goethite under this Cit concentration was similar to the 300 mg/L Cit system, with adsorption rates reaching 100% within 20 days. This indicates that Cit concentrations of 300 mg/L and 150 mg/L exerted limited influence on the adsorption system, resulting in nearly identical adsorption behaviors.

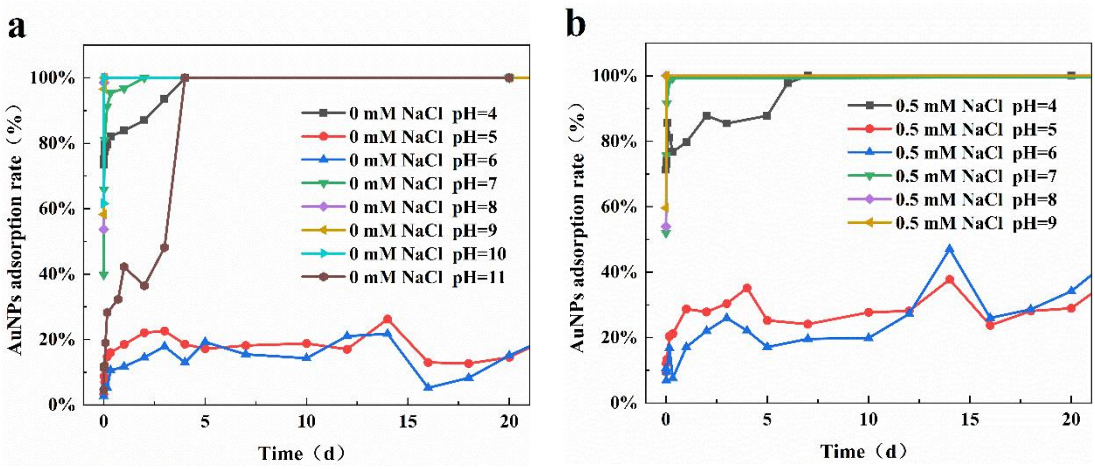

Figure 8. Adsorption Rate of AuNPs on Goethite over Time under Different Initial pH Values at a Cit Voncentration of 150 mg/L: (a) 0 mM NaCl; (b) 0.5 mM NaCl

3.2.3 Adsorption of AuNPs-75 on Goethite

This study also investigated the adsorption behavior of AuNPs on goethite under a Cit concentration of 75 mg/L across initial pH 4–11 (Figure 9). Results demonstrated that complete adsorption occurred within 8 hours, with adsorption rates increasing as Cit concentration decreased. The slowest adsorption rates were observed at pH 5, 6, and 11, consistent with findings under higher Cit concentrations. This phenomenon reveals that reducing Cit concentration enhances the adsorption capacity of goethite on AuNPs. While no significant differences were observed when Cit concentration decreased from 300 mg/L to 150 mg/L, a further reduction to 75 mg/L induced marked changes in adsorption behavior. This suggests the existence of a critical Cit concentration threshold influencing the adsorption system, located between 150 mg/L and 75 mg/L.

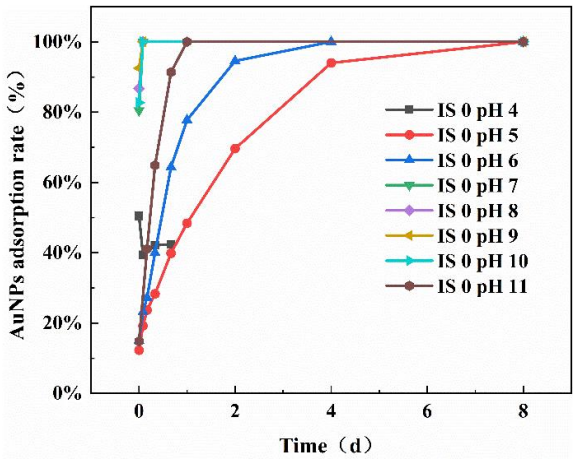

Figure 9. Adsorption Rate of AuNPs on Goethite over Time under Different Initial pH Values at a Cit Concentration of 75 mg/L (IS = 0 mM NaCl)

3.2.4 Adsorption of AuNPs-15 on Goethite

Under a Cit concentration of 15 mg/L, goethite exhibited remarkable adsorption capability for AuNPs across varying initial pH and IS conditions (Figure 10). The adsorption process was extremely rapid, with complete adsorption achieved within 5 minutes. Due to the ultrafast kinetics, pH exerted negligible influence on the adsorption process. Adsorption was already observed in the 0-minute sample (i.e., immediately after mixing AuNPs colloid with goethite). However, as sampling time could not be precisely controlled to the second, the specific impact of pH variation on adsorption kinetics could not be accurately evaluated.

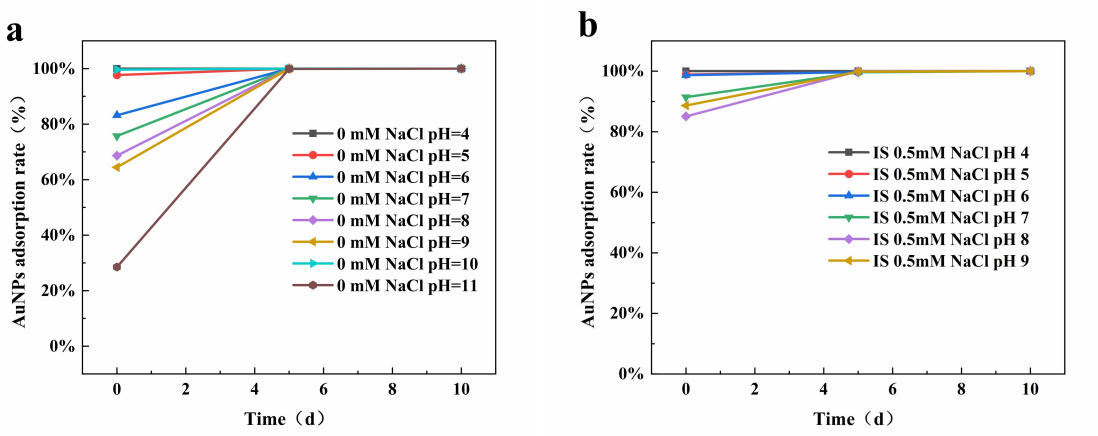

Figure 10. Adsorption Rate of AuNPs on Goethite over Time under Different Initial pH Values at a Cit Concentration of 15 mg/L: (a) 0 mM NaCl; (b) 0.5 mM NaCl

3.3 Desorption Characteristics and Reusability of Goethite

To evaluate the reusability of goethite, black floating objects were observed in the goethite-AuNPs system during desorption experiments as the desorption time increased. We hypothesize that these

substances represent AuNPs desorbed from goethite. Upon detachment, the AuNPs lost colloidal stability in solution, underwent intense homogeneous aggregation (evidenced by their characteristic black coloration), and floated on the suspension surface due to their relatively low density. Notably, these black floating aggregates (i.e., desorbed AuNPs) were detected across all tested initial pH conditions (pH 4–11) in the desorption systems.

Concurrently, Cit desorption behavior in the goethite-AuNPs adsorption system was investigated. Figure 10 illustrates the Cit desorption profiles under different initial pH conditions. The desorption patterns exhibited pH-dependent characteristics, which can be categorized into three distinct phases:

(1) In the pH 4–6 range, the desorbed Cit concentration increased with rising initial pH, reaching maximum desorption at pH 6.

(2) Between pH 7–9, desorption capacity progressively decreased with increasing pH.

(3) At alkaline conditions (pH 10–11), Cit desorption showed renewed enhancement as pH increased.

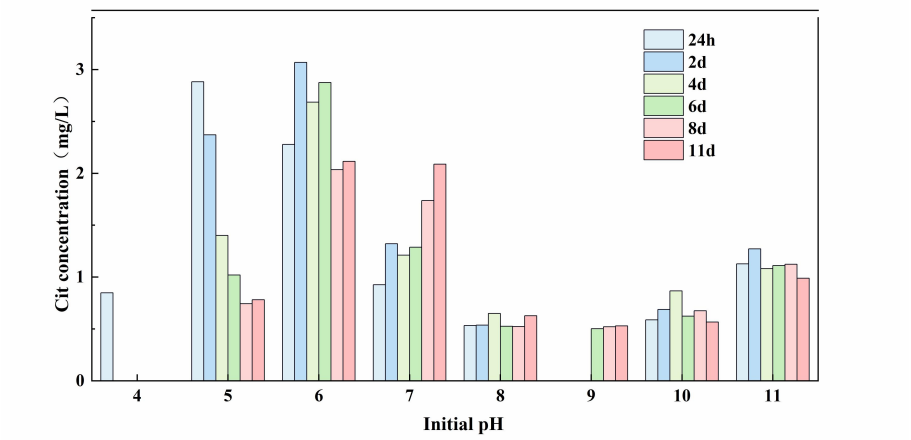

Figure 11. Concentration of Desorbed Cit in the Adsorption System under 300 mg/L Cit Conditions at Varying Initial pH Values

4. Discussion

4.1 Interactions of Cit with Goethite and AuNPs

4.1.1 Cit-Goethite Interaction

Batch adsorption experiments in the binary system (Citrate-goethite) revealed a significant decrease in Cit adsorption on goethite with increasing initial pH (Figure 12a). This pH-dependent behavior was consistently validated in the AuNPs-goethite ternary system (Figure 12b), demonstrating the universal pH dependence of Cit adsorption on goethite. According to Lindegren et al [33], Cit forms inner-sphere complexes under acidic/alkaline conditions but predominantly outer-sphere complexes at neutral pH. FTIR analysis further revealed that Cit adsorbs on goethite via bidentate coordination (central and terminal carboxyl groups), while hydroxyl groups and free carboxyl moieties participate in coordination at high pH, forming a tetradentate conformation. This coordination mechanism differs

markedly from Cit adsorption on AuNPs surfaces, potentially influencing competitive adsorption effects in complex systems (Park & Shumaker-Parry, 2014).

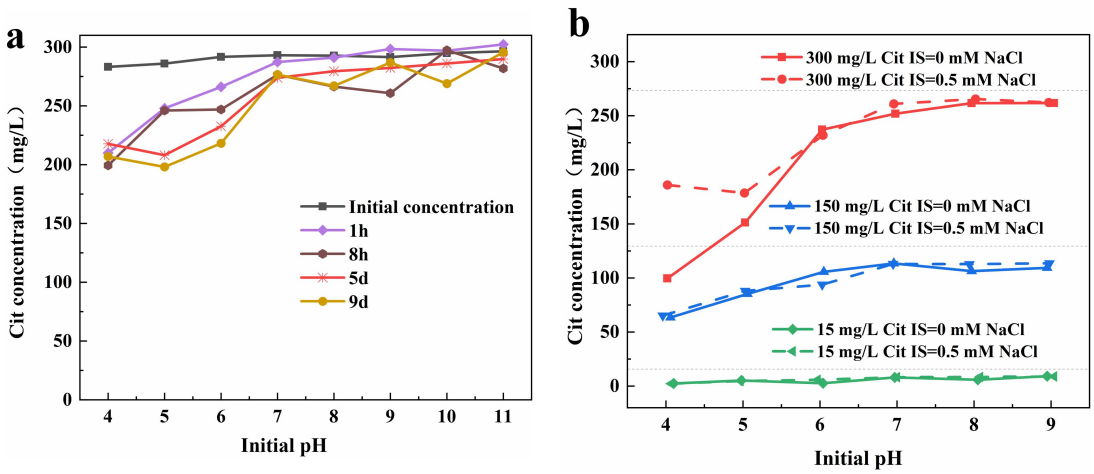

Figure 12. Concentration of Cit:(a) Cit Concentration not Adsorbed in the Adsorption Experiments of Goethite with Cit at Different Initial pH Conditions;(b) Cit Concentration Remaining in Solution at the End of Adsorption with Different Initial pH, IS, and Cit Concentration in Batch Adsorption Experiments

4.1.2 Differential Coordination of Cit with AuNPs

Cit pre-adsorbs on AuNPs surfaces during synthesis via mono-/bidentate coordination, transitioning to tetradentate coordination at pH ≥ 11 (Park & Shumaker-Parry, 2014). In contrast, Cit adsorption on goethite occurs dynamically at solid-liquid interfaces, exhibiting significantly reduced adsorption capacity under alkaline conditions exclusively through tetradentate coordination. This dynamic discrepancy suggests distinct adsorption sites and driving forces between goethite and AuNPs, providing critical insights into competitive adsorption phenomena in ternary systems.

4.2 Regulatory Mechanisms of Cit in Adsorption Systems

4.2.1 Competitive Adsorption and pH Dependence

Under alkaline conditions (pH 7–11), free Cit occupied <5% of goethite adsorption sites, showing negligible competition with AuNPs (Figure 12b). However, under acidic conditions (pH 4–6), Cit strongly occupied goethite surface sites, causing a sharp decline in AuNPs adsorption. Reducing Cit concentration to 15 mg/L attenuated competition, leading to significant AuNPs adsorption recovery. Notably, at pH 4, despite 80% Cit adsorption, AuNPs exhibited strong adsorption behavior. This anomaly may arise from Cit-induced surface charge reversal or site-specific adsorption mechanisms (e.g., inner-sphere complexation vs. edge hydroxyl binding) (Iglesias, López, Gondar, Antelo, Fiol, & Arce, 2010).

4.2.2 Critical Concentration Threshold

Experimental results (Section 3.2) demonstrated similar adsorption behaviors for goethite and AuNPs at Cit concentrations of 150 mg/L and 300 mg/L (Figures 6 and 8), with no concentration-dependent reduction in competition. However, at 75 mg/L Cit, adsorption behaviors diverged markedly (Figure 8), indicating a critical concentration threshold (~150 mg/L). This likely relates to dynamic adsorption-desorption equilibrium at interfaces: higher Cit concentrations stabilize adsorption layers via electrostatic repulsion and steric hindrance, while sub-threshold concentrations trigger destabilization through desorption dominance, releasing active sites for AuNPs adsorption (Westcott, Oldenburg, Lee, & Halas, 1998). These findings provide quantitative guidance for regulating nanoparticle-mineral interfacial behaviors.

4.3 Multiscale Analysis of Adsorption Mechanisms

4.3.1 pH-Driven Interfacial Interactions

Acidic conditions (pH 4–6): ATR-FTIR spectra (Figures 13-15) showed that the Carboxylic acid characteristic peak of citrate (e.g., vs(C=O) peak ~ 1713 cm-¹) were red-shifted after adsorption, indicating that hydrogen bonding dominated the adsorption (Lindegren, Loring, &Persson, 2009). Zeta potential analysis revealed electrostatic attraction between positively charged goethite (isoelectric point = 8.62) and negatively charged Cit/AuNPs. However, high Cit concentrations (≥150 mg/L) suppressed AuNPs adsorption via steric hindrance, peaking at pH 5–6 (Figure12b).

Alkaline conditions (pH 7–11): Despite electrostatic repulsion (both goethite and AuNPs being negatively charged) and reduced steric hindrance, adsorption rates remained high (60%). Second-derivative spectra displayed νas(COO^-) peak splitting (1585 → 1567 and 1611 cm^{-1}), suggesting charge-assisted hydrogen bond (CAHB) formation (Xu, Tran, Liu, Zhai, Wojtas, & Liu, 2024; Zhang, Lu, Liu, Guo, Sun, Jiang, & Song, 2025). Lewis acid-base interactions (goethite hydroxyls as bases vs. AuNPs carboxylates as acids) may synergistically drive adsorption (Zhao, Liu, Wang, Cao, & Xing, 2015).

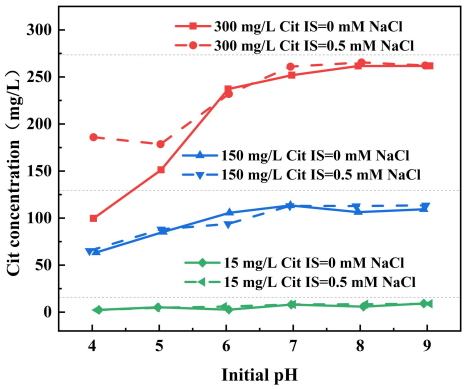

Figure 13. Variation of Adsorption Rate of Goethite on AuNPs with Initial pH when Adsorption Equilibrium is Reached in the Adsorption System

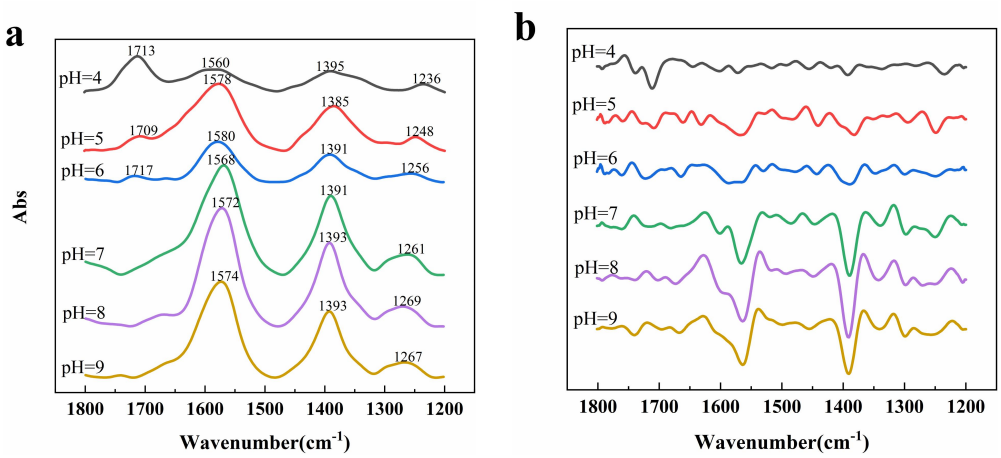

Figure 14. ATR-FTIR spectra of citrate with citrate at different pH conditions: (a) infrared spectra; (b) infrared second derivative spectra

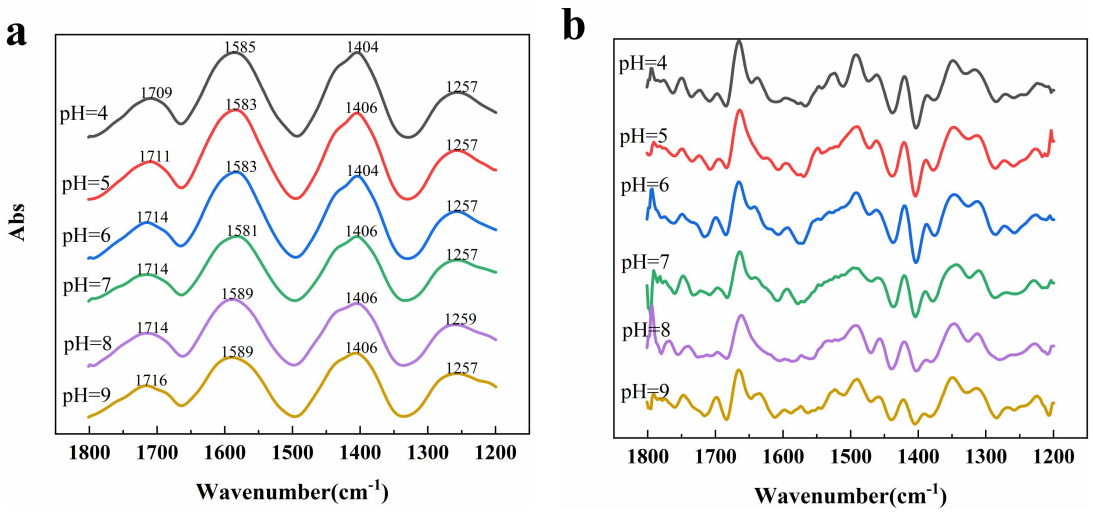

Figure 15. Difference Spectra of Citrate Adsorbed on Goethite after Adsorption of AuNPs Subtracted from the IR Spectra of Pure Goethite in Goethite Adsorbed with AuNPs Adsorption System: (a) IR Spectrogram; (b) Second-order Derivative Spectra

4.3.2 Dual Effects of Ionic Strength (IS)

IS compresses electrical double layers (reducing electrostatic attraction) while disrupting Cit hydrogen-bond networks (Wang, Nagata, Murano, & Pignatello, 2024). At pH 5–6 with 150 mg/L Cit, increasing IS from 0.01 M to 0.1 M enhanced adsorption by ~20%, attributable to hydrogen-bond suppression exposing active sites (Zhang, Chen, Liu, Li, Ge, & Ge, 2019). Conversely, at pH 4 with identical Cit concentration, IS elevation reduced adsorption by 15%, reflecting electrostatic dominance. This pH-dependent divergence aligns with surface coordination chemistry: higher protonation at low pH amplifies electrostatic interactions (Chen, 2021).

5.Conclusion

(1) **Cit regulation mechanism:** Cit competitively inhibits AuNPs adsorption on goethite in ternary systems (goethite-AuNPs- Citrate), predominantly under acidic conditions (pH 4–6). Reduced Cit concentrations weaken particle surface charge (lowering interparticle repulsion) and enhance AuNPs adsorption. The anomalous adsorption at pH 4 despite high Cit loading suggests altered binding modes (e.g., inner- This study systematically investigated Cit-mediated AuNPs adsorption on hydrothermally synthesized goethite, elucidating the impacts of pH, IS, and Cit concentration:

(2) **pH-driven mechanisms:**

- *Acidic conditions (pH 4–6):* Electrostatic attraction dominates at pH 4, while Cit-AuNPs competition prevails at pH 5–6.
- *Alkaline conditions (pH 7–11):* Synergistic effects of CAHB, van der Waals forces, and Lewis acid-base interactions drive strong AuNPs adsorption.

(3) **IS modulation:** IS exhibits dual effects—suppressing electrostatic interactions while disrupting hydrogen bonds. Dominant mechanisms shift with pH: hydrogen-bond suppression enhances adsorption at pH 5–6, whereas electrostatic weakening reduces adsorption at pH 4.

6. Outlook

The complex Cit-mediated adsorption mechanisms between goethite and AuNPs warrant further investigation. Future studies should employ advanced surface characterization techniques (e.g., extended X-ray absorption fine structure (EXAFS)) to elucidate atomic-scale adsorption structures and binding modes. Additionally, molecular dynamics simulations could provide deeper insights into competitive adsorption kinetics and interfacial processes.

Acknowledgments

This work was financially supported by the National Natural Science Foundation of China (42162006, 42163010), Guizhou Provincial Basic Research Program (Natural Science) (QKHJC [2020] 1Y171) and Guizhou Normal University Academic Seedling Fund (Qianshi Xinmiao No. 24)

Conflicts of Interest

The authors declare no conflicts of interest.

References

Huang, Y., Fan, C. Q., Dong, H., Wang, S. M., Yang, X. C., & Yang, S. M. (2017). Current applications and future prospects of nanomaterials in tumor therapy. *Int J Nanomedicine*, *12*, 1815-1825, https://doi.org/10.2147/IJN.S127349.

Chen, Y., & Feng, X. (2022). Gold nanoparticles for skin drug delivery. *International journal of pharmaceutics*, *625*, 122122. https://doi.org/10.1016/j.ijpharm.2022.122122

Zhang, Z., Cong, Y., Huang, Y., & Du, X. (2019). Nanomaterials-based Electrochemical Immunosensors. *Micromachines (Basel)*, *10*, 19. https://doi.org/10.3390/mi10060397

Li, C., Yang, J., Xu, R., Wang, H., Zhang, Y., & Wei, Q. (2022). Progress and Prospects of Electrochemiluminescence Biosensors Based on Porous Nanomaterials. *Biosensors*, *12*, 21. https://doi.org/10.3390/bios12070508

Staroverov, S. A., Vyrshchikov, R. D., Bogatyrev, V. A., & Dykman, L. A. (2024). The immunostimulatory roles of gold nanoparticles in immunization and vaccination against Brucella abortus antigens. *International Immunopharmacology*, *133*. https://doi.org/10.1016/j.intimp.2024.112121

Cai, Y., Li, M., Gu, J. J., Zhou, H., & Zhao, Y. (2021). An effective method for size-controlled gold nanoparticles synthesis with nonthermal microplasma. *Nanotechnology*, *32*, https://doi.org/10.1088/1361-6528/ac0d80

Kus-Liskiewicz, M., Fickers, P., & Ben Tahar, I. (2021). Biocompatibility and Cytotoxicity of Gold Nanoparticles: Recent Advances in Methodologies and Regulations. *International journal of molecular sciences*, *22*. https://doi.org/10.3390/ijms222010952

Zhang, Y., McKelvie, I. D., Cattrall, R. W., & Kolev, S. D. (2016). Colorimetric detection based on localised surface plasmon resonance of gold nanoparticles: Merits, inherent shortcomings and future prospects. *Talanta*, *152*, 410-422. https://doi.org/10.1016/j.talanta.2016.02.015

Koc, S. N. T., Benam, S. R., Aral, I. P., Shahbazi, R., & Ulubayram, K. (2024). Gold nanoparticles-mediated photothermal and photodynamic therapies for cancer. *International journal of pharmaceutics*, *655*.

Fernandez-Lopez, C., Polavarapu, L., Solis, D. M., Taboada, J. M., Obelleiro, F., Contreras-Caceres, R., Pastoriza-Santos, I., & Perez-Juste, J. (2015). Gold Nanorod-pNIPAM Hybrids with Reversible Plasmon Coupling: Synthesis, Modeling, and SERS Properties. *ACS applied materials & interfaces*, *7*, 12530-12538.

Wu, Y., Ali, M. R. K., Chen, K., Fang, N., & El-Sayed, M. A. (2019). Gold nanoparticles in biological optical imaging. *Nano Today*, *24*, 120-140. https://doi.org/10.1016/j.nantod.2018.12.006.

Dykman, L., Khlebtsov, B., & Khlebtsov, N. (2025). Drug delivery using gold nanoparticles. *Advanced Drug Delivery Reviews*, *216*.

Hochella, M. F., Mogk, D. W., Ranville, J., Allen, I. C., Luther, G. W., Marr, L. C., McGrail, B. P., Murayama, M., Qafoku, N. P., Rosso, K. M. et al. (2019). Natural, incidental, and engineered nanomaterials and their impacts on the Earth system. *Science*, *363*.

Miller, M. R., Raftis, J. B., Langrish, J. P., McLean, S. G., Samutrtai, P., Connell, S. P., Wilson, S., Vesey, A. T., Fokkens, P. H. B., Boere, A. J. F. et al. (2017). Inhaled Nanoparticles Accumulate at Sites of Vascular Disease. *ACS nano*, *11*, 4542-4552. https://doi.org/10.1021/acsnano.6b08551

Sharma, V. K., Filip, J., Zboril, R., & Varma, R. S. (2015). Natural inorganic nanoparticles – formation, fate, and toxicity in the environment. *Chemical Society Reviews*, *44*, 8410-8423.

https://doi.org/10.1039/c5cs00236b

Nie, X., Wan, Q., Hochella, M. F., Luo, S., Yang, M., Li, S., Fu, Y., Zeng, P., Qin, Z., & Yu, W. (2023). Interfacial adsorption of gold nanoparticles on arsenian pyrite: New insights for the transport and deposition of gold nanoparticles. *Chemical Geology*, *640*.

Stevenson, L. M., Dickson, H., Klanjscek, T., Keller, A. A., McCauley, E., & Nisbet, R. M. (2013). Environmental feedbacks and engineered nanoparticles: mitigation of silver nanoparticle toxicity to Chlamydomonas reinhardtii by algal-produced organic compounds. *PloS one*, *8*, e74456. https://doi.org/10.1371/journal.pone.0074456

Abbas, Q., Yousaf, B., Ullah, H., Ali, M. U., Ok, Y. S., & Rinklebe, J. (2020). Environmental transformation and nano-toxicity of engineered nano-particles (ENPs) in aquatic and terrestrial organisms. *Critical Reviews in Environmental Science and Technology*, *50*, 2523-2581. https://doi.org/10.1080/10643389.2019.1705721

Bebesi, T., Pálmai, M., Szigyártó, I. C., Gaál, A., Wacha, A., Bóta, A., Varga, Z., & Mihály, J. (2025). Surface-enhanced infrared spectroscopic study of extracellular vesicles using plasmonic gold nanoparticles. *Colloids and Surfaces B-Biointerfaces*, *246*. https://doi.org/10.1016/j.colsurfb.2024.114366

Wang, M., Gao, B., Tang, D., Sun, H., Yin, X., & Yu, C. Effects of temperature on aggregation kinetics of graphene oxide in aqueous solutions. *Colloids and Surfaces A: Physicochemical and Engineering Aspects*, *538*, 63-72. https://doi.org/10.1016/j.colsurfa.2017.10.061

Hanlie, H., Qinyan, W., Jianping, C., Shirong, L., & Ruizhong, H. (1999). Occurrence and distribution of invisible gold in the Shewushan supergene gold deposit, southeastern Hubei, China. *The Canadian Mineralogist*, *37*, 1525-1531.

Wu, J., Ye, Q., Li, P., Sun, L., Huang, M., Liu, J., Ahmed, Z., & Wu, P. (2023). The heteroaggregation behavior of nanoplastics on goethite: Effects of surface functionalization and solution chemistry. *Science of The Total Environment*, *870*. https://doi.org/10.1016/j.scitotenv.2023.161787

Smith, B. M., Pike, D. J., Kelly, M. O., & Nason, J. A. (2015). Quantification of Heteroaggregation between Citrate-Stabilized Gold Nanoparticles and Hematite Colloids. *Environ Sci Technol*, *49*, 12789-12797. https://doi.org/10.1021/acs.est.5b03486

Zhao, J., Liu, F., Wang, Z., Cao, X., & Xing, B. (2015). Heteroaggregation of Graphene Oxide with Minerals in Aqueous Phase. *Environmental Science & Technology*, *49*, 2849-2857. https://doi.org/10.1021/es505605w

Zhu, J., Fu, Q., Qiu, G., Liu, Y., Hu, H., Huang, Q., & Violante, A. Influence of low molecular weight anionic ligands on the sorption of heavy metals by soil constituents: A review. *Environmental Chemistry Letters*, *17*, 1271-1280. https://doi.org/10.1007/s10311-019-00881-1

Park, J. W., & Shumaker-Parry, J. S. (2014). Structural study of citrate layers on gold nanoparticles: role of intermolecular interactions in stabilizing nanoparticles. *Journal of the American Chemical Society*, *136*, 1907-1921. https://doi.org/10.1021/ja4097384

Grys, D. B., de Nijs, B., Salmon, A. R., Huang, J., Wang, W., Chen, W. H., Scherman, O. A., & Baumberg, J. J. (2020). Citrate Coordination and Bridging of Gold Nanoparticles: The Role of Gold Adatoms in AuNP Aging. *ACS nano*, *14*, 8689-8696. https://doi.org/10.1021/acsnano.0c03050

Enzweiler, J., & Joekes, I. (1992). Hetero- and homocoagulation of colloidal gold and iron oxides. *Journal of colloid and interface science*, *150*, 559-566.

Smith, B., Yang, J., Bitter, J. L., Ball, W. P., & Fairbrother, D. H. (2012). Influence of surface oxygen on the interactions of carbon nanotubes with natural organic matter. *Environ Sci Technol*, *46*, 12839-12847. https://doi.org/10.1021/es303157r

Fu, Y., Wan, Q., Qin, Z., Nie, X., Yu, W., & Li, S. (2020). The effect of pH on the sorption of gold nanoparticles on illite. *Acta Geochimica*, *39*, 172-180. https://doi.org/10.1007/s11631-020-00395-6

Frens, G. (1973). Controlled Nucleation for the Regulation of the Particle Size in Monodisperse Gold Suspensions. *Nature Physical Science*, *241*, 20-22. https://doi.org/10.1038/physci241020a0

Dhakal, P., Coyne, M. S., McNear, D. H., Wendroth, O. O., Vandiviere, M. M., D'Angelo, E. M., & Matocha, C. J. (2021). Reactions of nitrite with goethite and surface Fe(II)-goethite complexes. *The Science of the total environment*, *782*, 146406. https://doi.org/10.1016/j.scitotenv.2021.146406

Lindegren, M., Loring, J. S., & Persson, P. (2009). Molecular structures of citrate and tricarballylate adsorbed on alpha-FeOOH particles in aqueous suspensions. *Langmuir*, *25*, 10639-10647. https://doi.org/10.1021/la900852p

Iglesias, A., López, R., Gondar, D., Antelo, J., Fiol, S., & Arce, F. (2010). Adsorption of paraquat on goethite and humic acid-coated goethite. *Journal of hazardous materials*, *183*, 664-668, https://doi.org/10.1016/j.jhazmat.2010.07.077

Westcott, S. L., Oldenburg, S. J., Lee, T. R., & Halas, N. J. (1998). Formation and Adsorption of Clusters of Gold Nanoparticles onto Functionalized Silica Nanoparticle Surfaces. *Langmuir*, *14*, 5396-5401. https://doi.org/10.1021/la980380q

Xu, C., Tran, Q. G., Liu, D., Zhai, C., Wojtas, L., & Liu, W. (2024). Charge-assisted hydrogen bonding in a bicyclic amide cage: An effective approach to anion recognition and catalysis in water. *Chemical Science*, *15*, 16040-16049. https://doi.org/10.1039/d4sc05236f

Zhang, L., Lu, J., Liu, Q., Guo, Y., Sun, L., Jiang, R., & Song, X. (2025). An organic cage-based adsorbent for removing triphenylmethane dyes based on charge-assisted hydrogen bonding. *Journal of Environmental Chemical Engineering*, *13*. https://doi.org/10.1016/j.jece.2025.116028

Wang, Z., Nagata, M., Murano, H., & Pignatello, J. J. (2024). Participation of strong charge-assisted hydrogen bonds in interactions of dissolved organic matter represented by Suwannee River Humic Acid. *Water research*, *265*. https://doi.org/10.1016/j.watres.2024.122274

Zhang, X., Chen, L., Liu, R., Li, D., Ge, X., & Ge, G. (2019). The Role of the OH Group in Citric Acid

in the Coordination with Fe_3O_4 Nanoparticles. *Langmuir*, *35*, 8325-8332. https://doi.org/10.1021/acs.langmuir.9b00208

Chen, J. H. (2021). The interaction of flotation reagents with metal ions in mineral surfaces: A perspective from coordination chemistry. *Minerals Engineering*, *171*. https://doi.org/10.1016/j.mineng.2021.107067